Phenomenological theory of the transitions in the $(P(CH_3)_4)_2(CuCl_4)_{0.88}(CuBr_4)_{0.12}$ solid solution

1994 J. Phys.: Condens. Matter 6 849

(http://iopscience.iop.org/0953-8984/6/4/005)

J. Phys.: Condens. Matter 6 (1994) 849–858. Printed in the UK

Phenomenological theory of the transitions in the $[P(CH_3)_4]_2(CuCl_4)_{0.88}(CuBr_4)_{0.12}$ solid solution

D G Sannikov†, R Almairac, A Astito, J Moret, J Lapasset and P Saint Grégoire

Groupe de Dynamique des Phases Condensées (Laboratoire associée au CNRS 233), cc 26, Université Montpellier II, 34095 Montpellier Cédex 05, France

Received 23 April 1993

Abstract. A theoretical interpretation of the transition sequences in the $[P(CH_3)_4]_2(CuCl_4)_{1-x}(CuBr_4)_x$ solid solution is proposed. Each pure compound $[P(CH_3)_4]_2CuCl_4$ and $[P(CH_3)_4]_2CuBr_4$ presents its own transition sequence which contains an incommensurate phase and different locked phases. In the solid solution with $x = 0.12$, phases characteristic of the two pure compounds are observed in the sequence. The interpretation of this phase diagram is based on a coupling of the two order parameters, each of them corresponding to their own phonon branch. This coupling results in a re-entrant symmetry for one of the two order parameters, in agreement with experimental data.

1. Introduction

Two questions arise when undertaking a study of phase transitions in $A_{1-x}B_x$ solid solutions. The first concerns the homogeneity of the sample. As an example, if aggregates of B are present within the A matrix, then the properties of the sample can be described as a superposition of the properties of the two pure compounds. The second question is connected with the occurrence of long-range ordering. There presumably exists a limiting concentration x_L such that, for $x > x_L$, long-range correlations take place between the molecules of the chemical species B. Then for $x > x_L$ the solid solution behaves like a pure crystal with respect to the properties of both species. For $x < x_L$ the sample will behave as a pure crystal for the properties of only species A, B acting as impurities.

The phase diagram of the $[N(CH_3)_4]_2CuBr_xCl_{4-x}$ solid solution gives an example of such a homogeneous compound where long-range ordering is present [1]. The homogeneity is demonstrated by the continuous dependence of the transition temperatures on composition. This phase diagram results from competition between the order parameters of the two pure salts. For some composition ranges, ordering occurs simultaneously in both symmetry directions, i.e. for the two order parameters.

Analogous to the previous compound, $[P(CH_3)_4]_2(CuCl_4)_{1-x}(CuBr_4)_x$ where $x = 0.12$ is also an interesting example of a solid solution. It exhibits a complicated sequence of at least six phases between room temperature and 110 °C (table 1) [2]. Some of these phases present the same space group as in the pure bromide and others the same space group as in the pure chloride compound. The case of the two pure compounds is described in section 2

† Permanent address: Institute of Crystallography, Academy of Sciences, Leninski Precinct 59, 117333 Moscow, Russia.

0953-8984/94/040849+10$07.50

Table 1. Schematic representation of phase transition sequences in the compound $[P(CH_3)_4]_2(CuCl_4)_{1-x}(CuBr_4)_x$ with different x($x = 1$ is the pure Br compound; $x = 0$ is the pure Cl compound).

Solid solution x= 0.12

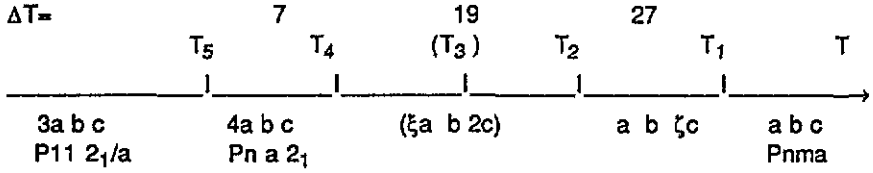

x= 1 pure Bromide compound

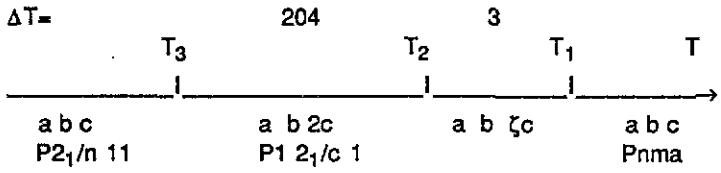

x= 0 pure Chloride compound

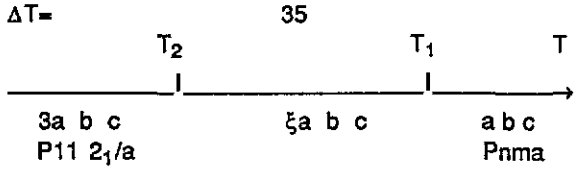

of the present paper where we give the phenomenological interpretation of the transition sequences and compare them with available experimental data.

In the solid solution with $x = 0.12$, despite the low value of x, long-range ordering occurs simultaneously in the a and c directions which are characteristic of the $CuCl_4$ [3] and $CuBr_4$ [4] species, respectively. Consequently a phenomenological theory of the transition sequence in this compound must take into account the order parameters of both the two pure salts. All through this work we use the language of lattice dynamics. The term 'soft mode' is used because it gives an understandable description of the different situations. Nevertheless, one should keep in mind that the mechanism of the transition is perhaps not

of the displacive type. The phenomenological theory presented in section 3 for the solid solution applies to a pure crystal where two sets of order parameters are in competition.

Finally a short discussion, containing an analysis of the results obtained within the present theory, is given in section 4.

2. Phenomenological theory of the transitions in the pure compounds

2.1. $[P(CH_3)_4]_2CuBr_4$

From DSC measurements it was found that the high-temperature phase transition at about 135° in $[P(CH_3)_4]_2CuBr_4$ was either of first order or continuous but close to tricritical point. Close to this temperature we obtained evidence of an intermediate incommensurate phase extending over a temperature range of about 3 K because of the presence in the free-energy expansion of a Lifshitz term [4].

Now we wish to improve the phenomenological treatment of phase transitions in this compound so as to interpret the whole transition sequence which includes four different phases. To achieve this we shall see that it is sufficient to consider the single soft optical branch of the normal vibration spectrum.

The symmetry of this branch is unambiguously determined since the symmetry group of the low-temperature phase with the same translational symmetry (abc) as in the initial phase $Pnma$ (D_{2h}^{16}) is known. It is $P2_1/n11$ and it is induced by the representation $B_{3g}(yz)$ of the point group D_{2h} (see, e.g., [5]). Therefore the coordinate of the mode with the wavevector $q = 0$ transforms with respect to the representation B_{3g}. This determines the symmetry of the corresponding branch. From the tables of space groups of commensurate phases for the initial phase of the space group D_{2h}^{16} [5], it follows that the possible space groups of the phase with $q_c = \frac{1}{2}$ ($q = q_c c^*$) are $P12_1/c_1$ or $P2_1ca$ (also possible, but less probable, is the group $P1c1$). The first of these possibilities corresponds to the experimental data (see table 1).

The soft branch is represented by the simple expression

$$\alpha(q) = A + \kappa(q^2 - B^2)^2 \tag{1}$$

where α is the elastic coefficient of the normal vibration associated to the branch, and A and B are coordinates of the minimum of the branch (1) (figure 1(a)).

The phase diagram obtained using the method proposed in [6, 7], is shown in figure 2. Along the axes we plot the parameters A and B of the soft mode, i.e. of the minimum of the soft branch, in the dimensionless variables

$$x = B/Q \qquad y = -A/\kappa Q^4. \tag{2}$$

Here Q has the dimension of a wavevector the value of which can be chosen arbitrarily. It is convenient to take it equal to the value of the Brillouin zone boundary $Q = \frac{1}{2}$ (in units of c^*). κ characterizes the steepness of the branch in the vicinity of the minimum (see figure 1(a)).

Each commensurate phase, i.e. the phases corresponding to rational values of the wavevector $q_l = m/l$, where m and l are integers, can be characterized by the dimensionless parameter

$$\epsilon_l = (|\alpha_l'|/\kappa Q^4)(\kappa Q^4/2\beta)^{l-1} \tag{3}$$

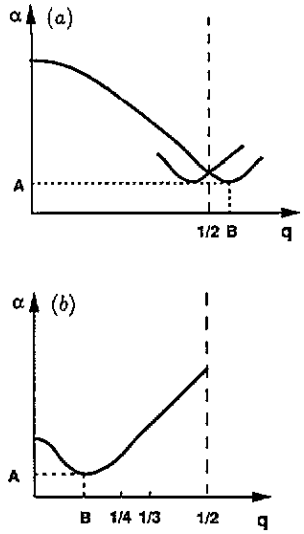

Figure 1. (*a*) Optical soft branch, i.e. the dependence of the elastic coefficient $\alpha \sim \omega^2$ (ω is the frequency) on the wavevector q (in units of $2\pi/c$) along the c^* direction for the pure Br compound. (*b*) Optical soft branch showing the dependence of $\alpha(q)$ with q (in units $2\pi/a$) along the a^* direction for the pure Cl compound.

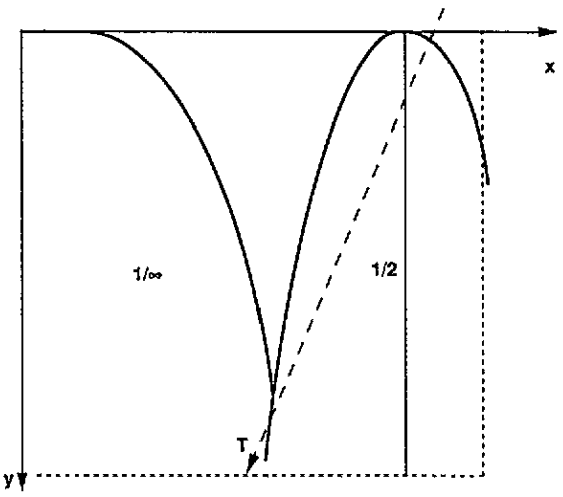

Figure 2. Phase diagram on the (x, y) plane (see equation (2) in the text) for the pure Br compound. The phase trajectory with decreasing temperature is shown by the broken arrow. The wavevectors of the commensurate phases $q = 1/m$, are indicated.

which involves the coefficients of the thermodynamic potential for the rational values of $q_l = m/l$:

$$\Phi_l = \alpha_l \rho^2 + \beta \rho^4 - \alpha_l' \rho^{2l} \cos(2l\phi) \tag{4}$$

where the elastic coefficient α_l depends on q according to equation (1):

$$\alpha_l = A + \kappa(q_l^2 - B^2)^2$$

and ρ and ϕ are the amplitude and phase of the two-component order parameter, i.e. the coordinates of the two-degenerate mode of the branch ($\alpha(q) = \alpha(-q)$). Note that, the larger ϵ_l is, the wider at a fixed value of Q is the range of existence of the corresponding commensurate phase in the phase diagram of figure 2 (see also figure 3).

In figure 2 we use the value $\epsilon_2 = 0.3$. The phase trajectory is chosen in such a way as to obtain the correspondence first to the observed sequence of phase transitions, second to the approximate ratio of temperature ranges of existence of the incommensurate phase (3 K) and of the commensurate phase with $q = \frac{1}{2}$ (204 K), and third to the dependence of the misfit parameter on temperature T in the incommensurate phase [2, 4] ($q \simeq 0.524$ at T_i and at the lock-in transition it jumps from $q \simeq 0.517$ to $q = \frac{1}{2}$).

2.2. $[P(CH_3)_4]_2CuCl_4$

Table 1 also shows the phase transition sequence in the compound $[P(CH_3)_4]_2CuCl_4$. According to tables in [5], such a sequence of phase transitions can be described by a

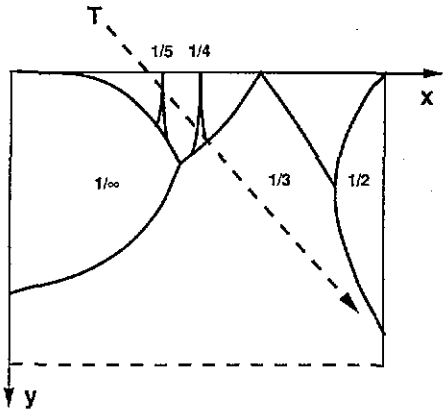

Figure 3. Phase diagram on the (x, y) plane (see equation (2) in the text) for the pure Cl compound. The broken arrow indicates the phase trajectory with decreasing temperature.

single optical branch. The mode with $q = 0$, which belongs to this branch, can transform with respect to the representation either B_{3g} (yz) or A_u (xyz) of the point group D_{2h}. To these representations correspond the space groups $P2_1/n11$ and $P2_12_12_1$, respectively (with the equitranslational cell abc). However, up to now, no transition to a low-temperature equitranslational phase has been experimentally evidenced.

The expression for the soft branch $\alpha(q)$ can be presented in the same form as before (equation (1)), but now all quantities are different (e.g. $q = q_x a^*$). The dependence $\alpha(q)$ is shown schematically in figure 1(b).

In figure 3 the phase diagram corresponding to this branch is given. It is plotted in the same way as for the diagram in figure 2. We use the following values of ϵ_l (see (3) for a definition of ϵ_l): $\epsilon_3 = 1$, $\epsilon_2 = 0.2$, $\epsilon_4 = 0.02$ and $\epsilon_5 = 0.1$.

This choice is connected with the slope of the phase trajectory which corresponds to the experimental dependence of the misfit parameter on temperature in the incommensurate phase [3] ($q \simeq 0.18$ at T_i; it increases to $q \simeq 0.26$ at T_c and jumps to the value $q = \frac{1}{3}$). The phase trajectory crosses the commensurate phase with $q = \frac{1}{5}$; however, this phase can be very narrow and on the scale of figure 3 has almost no width. The trajectory also crosses the commensurate phase with $q = \frac{1}{4}$. The value $\epsilon_4 = 0.02$ was chosen to be so small that this phase is narrow in the diagram. However, in principle, this phase must be observed in experiment as some narrow plateau in the dependence $q(T)$.

The space group of the phase with $q = \frac{1}{4}$, in accordance with the tables in [5] can be either $Pna2_1$ or $P12_1/a1$. In the first case the electric field along the z axis must broaden the range of existence of the phase with $q = \frac{1}{4}$. Then this phase must be more reliably observed in experiment.

3. Phenomenological interpretation of the transition sequence in a solid solution

On the basis of table 1, one can guess that in solid solution with $x = 0.12$ a condensation of both order parameters, i.e. of the Cl and of the Br compound, occurs. In the framework of our phenomenological interpretation, two soft phonon branches which are characteristic of the pure compounds simultaneously exist. Note that from symmetry considerations the symmetry group of a mixed phase contains only the common elements of the two original

symmetry groups. In this respect, as the low-temperature phase of the solid solution with $x = 0.12$ is the same as in the pure chloride compound, the influence of the bromide salt no longer applies in this temperature range. This means that the soft branch responsible for the c direction ordering condenses at high temperatures but in the low-temperature range the condensation of this mode no longer takes place. This can happen if the corresponding soft mode first decreases (and therefore the elastic coefficient becomes negative) and then increases (and the elastic coefficient again becomes positive). We suppose that this can occur owing to the interaction of the two branches of the crystal lattice. Let us consider this hypothesis in more detail.

The thermodynamic potential for the soft branch along the c^* axis can be written in the form

$$\Phi_c = \alpha_c \rho_c^2 + \beta_c \rho_c^4 \tag{5}$$

where ρ_c is now the amplitude of the first two-component order parameters in the solid solution.

For rational numbers of q, $q_l = m/l$ where m and l are integers, we must add to the potential (5), as was done in equation (4), the invariants $\alpha_c' \rho_c^{2l} \cos(2l\phi_c)$, where ϕ_c is the phase of the order parameter. However, in the weak-anisotropy approximation which is used here these invariants are small in comparison with the invariant $\beta_c \rho_c^4$ and we may neglect them in what follows.

We suppose that only the coefficient α_c (but not the coefficient β_c) depends on temperature T and on the wavevector q_c:

$$\alpha_c(q_c) = A_c + \kappa_c(q_c^2 - B_c^2)^2 \tag{6}$$

where the coordinates A_c and B_c of the minimum of the branch (6) depend on T linearly:

$$A_c = A_{cT}(T - T_c) \qquad B_c = B_{cT}T. \tag{7}$$

For the soft branch along the a^* axis we use the same assumptions:

$$\begin{aligned} &\Phi_a = \alpha_a \rho_a^2 + \beta_a \rho_a^4 \\ &\alpha_a(q_a) = A_a + \kappa_a(q_a^2 - B_a^2)^2 \\ &A_a = A_{aT}(T - T_a) \qquad B_a = B_{aT}T. \end{aligned} \tag{8}$$

The full thermodynamic potential Φ is the sum of the two potentials (5) and (8) and it also contains an interaction term which is proportional to the constantly existing invariant $\rho_c^2 \rho_a^2$ (a similar potential has been used previously; see [9]):

$$\Phi = A_c \rho_c^2 + \beta_c \rho_c^4 + A_a \rho_a^2 + \beta_a \rho_a^4 + 2b\rho_c^2 \rho_a^2. \tag{9}$$

Here we replace α_c by A_c and α_a by A_a. For an incommensurate phase it is possible to do so, since the condition for the potential(s) (5) (and (8)) to be minimum is realized by the equality $q_c = B_c$ ($q_a = B_a$). For a commensurate phase where $q = q_{cl}$ the term $\kappa_c(q_{cl}^2 - B_c^2)^2$ is small in comparison with A_c owing to the weak-anisotropy approximation and hence we may assume that $\alpha_c = A_c$ in what follows. To make the potential (9) finite we must assume that $\beta_c > 0$, $\beta_a > 0$ and $\beta_a\beta_c - b^2 > 0$. We suppose also that $b > 0$.

With decreasing temperature the coefficient A_c in the potential (9) first vanishes at $T = T_c$ and the spontaneous value of the amplitude ρ_c arises:

$$\rho_c^2 = -A_c/2\beta_c \qquad \Phi = -A_c^2/4\beta_c + \tilde{A}_a \rho_a^2 + \beta_a \rho_a^4 \qquad \tilde{A}_a = A_a - (b/\beta_c)A_c. \tag{10}$$

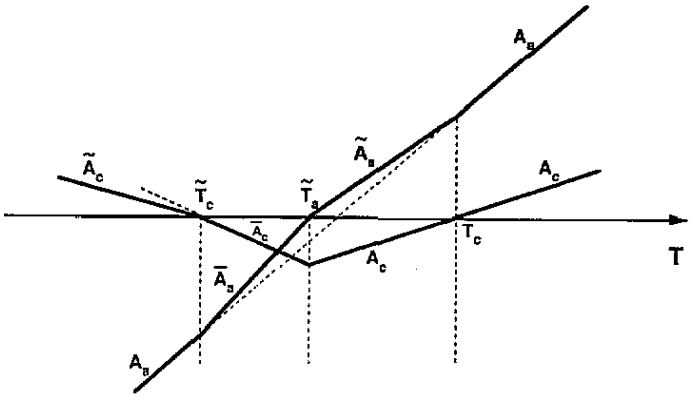

Figure 4. Dependences of the coefficients A_c, A_a, $\tilde{A}_a$, $\bar{A}_c$,$\bar{A}_a$ and $\tilde{A}_c$ on temperature T (see equation (11)–(13)).

As can be seen from equations (10), the coefficient of ρ_a^2 is renormalized owing to the interaction term in the potential (9) and we obtain

$$\tilde{A}_a = \tilde{A}_{aT}(T - \tilde{T}_a) \qquad \tilde{A}_{aT} = A_{aT} - (b/\beta_c)A_{cT}. \tag{11}$$

The slope $\tilde{A}_{aT}$ of the temperature dependence of $\tilde{A}_a(T)$, although decreasing, remains positive: $0 < \tilde{A}_{aT} < A_{aT}$ and $\tilde{T}_a < T_a$ (figure 4).

At $T = \tilde{T}_a$ the coefficient $\tilde{A}_a$ in the potential (10) vanishes in turn and the spontaneous value of the amplitude ρ_a arises in addition to the spontaneous value of ρ_c:

$$\begin{aligned} &\rho_a^2 = -\bar{A}_a/2\beta_a \qquad \rho_c^2 = -\bar{A}_c/2\beta_c \qquad \bar{A}_a = \tilde{A}_a/(1 - b^2/\beta_a\beta_c) \\ &\bar{A}_c = \tilde{A}_c/(1 - b^2/\beta_a\beta_c) \qquad \tilde{A}_c = A_c - (b/\beta_a)A_a. \end{aligned} \tag{12}$$

Here both coefficients are renormalized and we obtain

$$\begin{aligned} &\bar{A}_a = \bar{A}_{aT}(T - \tilde{T}_a) \qquad \bar{A}_c = \bar{A}_{cT}(T - \tilde{T}_c) \\ &\bar{A}_{aT} = \tilde{A}_{aT}/(1 - b^2/\beta_a\beta_c) \qquad \bar{A}_{cT} = \tilde{A}_{cT}/(1 - b^2/\beta_a\beta_b). \end{aligned} \tag{13}$$

However, now the slope $\bar{A}_{cT}$ of the dependence $\bar{A}_c(T)$ and hence the slope $\tilde{A}_{cT}$ of the dependence $\tilde{A}_c(T)$, becomes negative: $\bar{A}_{cT} < \tilde{A}_{cT} < 0$ (see figure 4). This supposes that the condition $A_{cT} < A_{aT}b/\beta_a$ is fulfilled. Note that from a comparison of the experimental data presented in figures 2 and 4 of [8] we may conclude that the slope $\bar{A}_{aT}$ is approximately twice the slope A_{cT}.

At $T = \tilde{T}_c$ the spontaneous value of ρ_c (12) vanishes and for $T < \tilde{T}_c$ we obtain

$$\rho_a^2 = -A_a/2\beta_a. \tag{14}$$

Thus, starting from the initial phase, we obtain: no ordering in the initial phase ($T > T_c$); ordering along the c axis in the range $\tilde{T}_a < T < T_c$; both ordering along the a and c axes in the range $\tilde{T}_c < T < \tilde{T}_a$; and ordering along the a axis only, for $T < \tilde{T}_c$.

Now we must superimpose these three second-order phase transitions at $T = T_c$, $T = \tilde{T}_a$ and $T = \tilde{T}_c$ on the phase transitions which are connected with crossing boundaries between

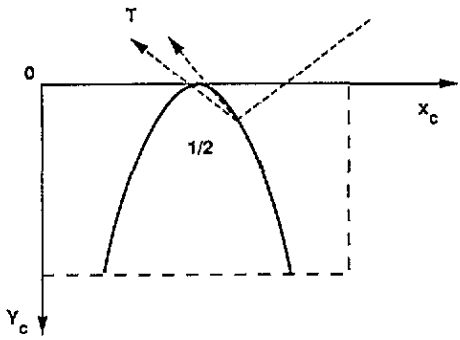

Figure 5. Part of the phase diagram on the (x_c, y_c) plane near the point $x_c = \frac{1}{2}$ for the solid solution with $x = 0.12$. The phase trajectory (two variants) with the re-entrant behaviour is shown by the broken arrow (compare with the phase diagram in figure 2 for the pure Br compound).

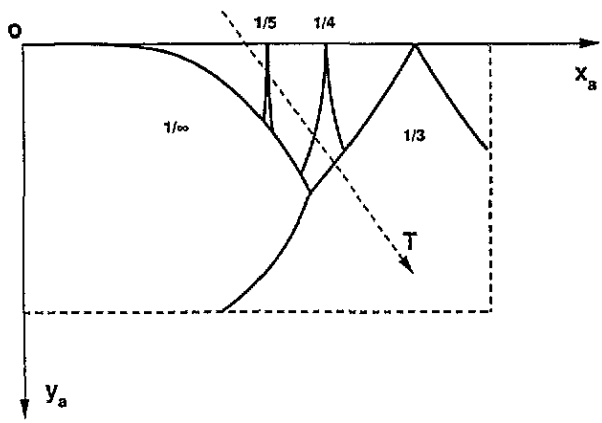

Figure 6. Part of the phase diagram on the (x_a, y_a) plane in the vicinity of the points $x_a = \frac{1}{5}, \frac{1}{4}$ and $\frac{1}{3}$ for the solid solution with $x = 0.12$. The phase trajectory is shown by the broken arrow (compare with figure 3 for the pure Cl compound).

different incommensurate and commensurate phases by phase trajectories on the phase diagrams (A_c, B_c) and (A_a, B_a).

Figures 5 and 6 present parts of the phase diagrams (A_c, B_c) and (A_a, B_a), respectively, in the dimensionless variables $x_c = B_c/Q$ and $y_c = A_c/\kappa_c Q^4$ ($x_a = B_a/Q$ and $y_a = A_a/\kappa_a Q^4$). These diagrams are plotted in such a way that the differences between them and the similar phase diagrams for the pure compounds (see figures 2 and 3) are as small as possible while the agreement with available experimental data is as good as possible. Note that the slopes of the phase trajectories on the diagrams in figure 5 and 6 correspond to the slopes of the dependences on the coefficients A, $\tilde{A}$ and $\tilde{A}$ on T in figure 4. (Indeed, for example, from equation (7) it follows that $A_c \sim B_c A_{cT}/B_{cT}$.) However, for simplicity, only the kink at $T = \tilde{T}_a$ is shown in figure 5 and no kink is shown in figure 6.

In figure 5 we assume that $\epsilon_2 = 0.3$, i.e. it has the same value as for the pure compound. The initial slope of the phase trajectory is chosen in such a way that it corresponds to the dependence of the misfit parameter on temperature (see figure 2 in [8]). When this trajectory crosses the boundary between the incommensurate phase and the commensurate phase with

$q_c = \frac{1}{2}$, the phase transition between these phases occurs at $T = T_c'$.

As follows from table 1, the phase transition from the initial phase ($Pnma$) into the incommensurate phase along the c axis ($a\,b\,\zeta c$) occurs at $T = T_1$ and hence $T_1 = T_c$. At $T = T_2$ the phase transition into the phase ($\xi a\,b\,2c$) is observed. Here we have simultaneously two transitions: one from (a) to (ξa) at $T = \tilde{T}_a$ and the other from (ζc) to ($2c$) at $T = T_c'$ and hence $\tilde{T}_a = T_c'$. The coincidence of two transitions is possible since one of these transitions at $T = T_c'$ is of the first order. It is possible also that the temperatures $\tilde{T}_a$ and T_c' do not coincide but are so close to each other that they are not distinguished by experiment. In this case it would be possible to observe in the vicinity of $T = T_2$ a phase with the parameters ($a\,b\,2c$) if $\tilde{T}_a < T_c'$ or ($\xi a\,b\,\zeta c$) if $\tilde{T}_a > T_c'$. If $T_2 = \tilde{T}_a = T_c'$ the kink of the phase trajectory accordingly coincides with the crossing by the trajectory of the boundary in figure 4. At this point the phase trajectory changes its direction from going downwards to going upwards and the re-entrant part of the trajectory begins. In figure 5 we show two variants of such a trajectory since both possibilities are not in contradiction with the experimental data. A steeper slope of the trajectory is in greater agreement with the data since the temperature range of the existence of the commensurate phase with $q_c = \frac{1}{2}$ (19°; see table 1) is less than that of the incommensurate phase (27°; see table 1).

With further decreasing temperature the re-entrant trajectory in figure 5 crosses two boundaries between the phases commensurate with $q_c = \frac{1}{2}$, incommensurate and initial with respect to the ordering along the c axis, and two corresponding phase transitions occur. However, as can be seen from figure 5, the range of existence of the incommensurate phase is very narrow and this phase could hardly be observed in experiment. Then the transition from (2c) to (c) occurs at $T = \tilde{T}_c$. At $T < \tilde{T}_c$ the ordering along the c axis no longer exists and the crystal returns to the initial symmetry with respect to this ordering.

The re-entrant behaviour of the trajectory in figure 5 can explain the unusual temperature dependence of the integrated intensity of the satellite reflection (see figure 1 in [8]). This intensity instead of increasing with decreasing temperature, reaches a maximum at $T \lesssim T_2$ and then begins to decrease down to zero level.

In figure 6 the initial slope of the phase trajectory is chosen in accordance with the experimental dependence of the misfit parameter along a^* on temperature (see figure 4 in [8]). The values $\epsilon_4 = 0.1$ and $\epsilon_3 = 0.7$ are chosen in such a way that the temperature ranges of the existence of the incommensurate phase along the a axis and of the commensurate phase with $q_a = \frac{1}{4}$ correspond approximately to the experimental data 19° and 7°, respectively (see table 1). Note that the choice of values for ϵ_4 and ϵ_3 in figure 6 and for ϵ_2 in figure 5 is not so strict. Note also that experimental data of the phases in the range $T_4 < T < T_2$ are not definitively established. Therefore in this consideration we neglect the existence of the phase transition at $T = T_3$.

As follows from table 1, at $T = T_4$ we have simultaneously two transitions: one from (2c) to (c) at $T = \tilde{T}_c$ and the other from (ξa) to ($4a$) at $T = T_a'$ (cf the case of phase transition at $T = T_2$). Therefore $\tilde{T}_c = T_a'$ and the two transitions coincide. Such a coincidence is possible since one of these transitions at $T = T_a'$ is of first order. It is possible also that the temperatures $\tilde{T}_c$ and T_a' are so close to each other that they are not distinguished in experiment. In this case in the vicinity of $T = T_4$ some additional phases could be observed, e.g. with the parameters ($\xi a\,b\,\zeta c$) and ($\xi a\,b\,c$) if $T_a' < \tilde{T}_c$ or ($4a\,b\,2c$) and ($4a\,b\,\zeta c$) if $T_a' > \tilde{T}_c$.

If $T_4 = \tilde{T}_c = T_a'$, the phase with the parametrs ($4a\,b\,c$) exists at $< T_4$. The space group of this phase must be determined only by the soft branch along the a axis, i.e. it must be the same as in the pure chloride compound, namely $Pna2_1(4a\,b\,c)$, and it is exactly what is observed in experiment (see table 1).

The last phase transition occurs at $T = T_5$ when the phase trajectory in figure 6 crosses the boundary between the two commensurate phases with $q_a = \frac{1}{4}$ and $q_a = \frac{1}{3}$. The phase at $T < T_5$ must have the parametrs $(3a\,b\,c)$ and the space group $P112_1/a$ as in the pure chloride compound which again coincides with experiment (see table 1).

4. Conclusion

Further experimental data are necessary to check the theoretical treatment given above, and in particular experiments which should clarify the T_2 and T_3 transitions. It would be also very interesting to measure the phase diagram of solid solutions with different x, especially with x less than 0.12. With decreasing x the phase transition temperatures T_c and T_a in figure 4 become closer to each other and, at some critical value $x = x_0$, they should coincide. At $x < x_0$, only ordering along the a axis occurs (figure 7). With decreasing x, interactions between Br ions decrease and the long range order in the arrangement of Br ions can be lost; then $x = x_L$. If x_L is less than x_0, then on the (x, T) phase diagram the tetracritical point must be observed on the phase transition line from the initial phase to the lower temperature phases.

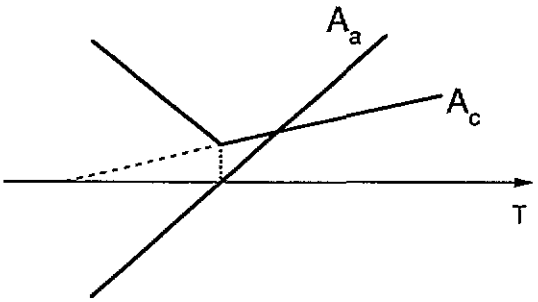

Figure 7. Dependences of the coefficients A_c and A_a on temperature T in the case $x < x_0$ (see text).

In this point $(x = x_0)$, ordering along the c axis no longer takes place. A similar tetracritical point was observed for the $[N(CH_3)_4]_2CuBr_xCl_{4-x}$ solid solution (at $x \simeq 1.8$ [1]). On the contrary, if x_L is greater than x_0, then the tetracritical point cannot be observed on the (x, T) phase diagram.

References

[1] Liechti O, Perret R and Arend H 1986 *Solid State Commun.* **60** 223
Liechti O, Kind R, Preslovsek P, Filipic C and Levstik A 1991 *Phys. Rev.* B **44** 7209
[2] Almairac R, Astito A, Lapasser J, Moret J and Saint Grégoire P 1992 *Ferroelectrics* **125** 203
[3] Pressprich M R, Bond M R, and Willet R D 1989 *Phys. Rev.* B **39** 3453
[4] Saint Grégoire P, Almairac R, Astito A, Lapasset J and Moret J 1991 *Solid State Commun.* **80** 451
[5] Sannikov D G 1991 *Kristallografia* **36** 813 (Engl. Transl. 1991 *Sov. Phys.–Crystallogr.* **36** 455)
[6] Sannikov D G 1989 *Zh. Eksp. Teor. Fiz.* **96** 2197 (Engl. Transl. 1989 *Sov. Phys.–JETP* **69** 1244)
[7] Sannikov D G 1990 *Zh. Eksp. Teor. Fiz.* **97** 2024 (Engl. Transl. 1990 *Sov. Phys.—JETP* **70** 1144)
[8] Astito A, Almairac R, Lapasset J, Saint Grégoire P and Moret J 1993 *Ferroelectrics* **141** 19
[9] Tolédano P, Pascoli G and Coiret M 1981 *J. Physique Coll.* **12** C6 746
See also
Holakovski J 1973 *Phys. Status Solidi* b **56** 615